



Supramolecular Fluorescence Probe Based on Twisted Cucurbit[14]uril for Sensing Fungicide Flusilazole

Ying Fan^{1,2}, Rui-Han Gao², Ying Huang², Bing Bian³, Zhu Tao^{2*} and Xin Xiao^{2*}

¹ State Key Laboratory Breeding Base of Green Pesticide and Agricultural Bioengineering, Key Laboratory of Green Pesticide and Agricultural Bioengineering, Ministry of Education, Guizhou University, Guiyang, China, ² Key Laboratory of Macrocyclic and Supramolecular Chemistry of Guizhou Province, Guizhou University, Guiyang, China, ³ College of Chemical and Environmental Engineering, Shandong University of Science and Technology, Qingdao, China

OPEN ACCESS

Edited by:

Angela Casini,
Cardiff University, United Kingdom

Reviewed by:

Dong-Sheng Guo,
Nankai University, China
Simin Liu,
Wuhan University of Science and
Technology, China

*Correspondence:

Zhu Tao
gzutao@263.net
Xin Xiao
gyhxxiaoxin@163.com

Specialty section:

This article was submitted to
Supramolecular Chemistry,
a section of the journal
Frontiers in Chemistry

Received: 30 August 2018

Accepted: 01 March 2019

Published: 21 March 2019

Citation:

Fan Y, Gao R-H, Huang Y, Bian B,
Tao Z and Xiao X (2019)
Supramolecular Fluorescence Probe
Based on Twisted Cucurbit[14]uril for
Sensing Fungicide Flusilazole.
Front. Chem. 7:154.
doi: 10.3389/fchem.2019.00154

The host-guest complex of the common dye, thioflavin T (ThT), and twisted cucurbit[14]uril (tQ[14]) was selected as a fluorescent probe to determine non-fluorescent triazole fungicides, including flusilazole, azaconazole, triadimefon, tebuconazole, tricyclazole, flutriafol, penconazole, and triadimenol isomer A, in an aqueous solution. The experimental results reveal that the ThT@tQ[14] probe selectively responded to flusilazole with significant fluorescence quenching and a detection limit of 1.27×10^{-8} mol/L. In addition, the response mechanism involves not only a cooperation interaction—ThT occupies a side-cavity of the tQ[14] host and the triazole fungicide occupies another side-cavity of the tQ[14] host—but also a competition interaction in which both ThT and the triazole fungicide occupy the side-cavities of the tQ[14] host.

Keywords: twisted cucurbit[14]uril, thioflavin T, fluorescent probe, triazole fungicides, flusilazole

INTRODUCTION

Triazole systemic fungicides, particularly flusilazole (1-[[bis(4-fluorophenyl) (methyl)silyl] methyl]-1*H*-1,2,4-triazole), are widely used in fruit, vegetable, and grain crops during cultivation and storage with high efficiency and good sterilization ability (Figure 1) (Zhang Y. H. et al., 2016). However, they still have somewhat toxic or other undesirable side effects on non-target organisms. Extensive or inappropriate use can cause soil and water pollution, and thus threaten human health (Ma et al., 2016). Therefore, it is necessary to develop sensitive and selective methods for the analysis of triazole fungicides, which are usually present in trace amounts.

The most common analytical method used for the trace determination of triazoles, particularly flusilazole residues in water, is chromatography e.g., liquid chromatography-tandem mass spectrometry (LC-MS/MS) (García-Valcárcel and Tadeo, 2011; Fu et al., 2017), high-performance liquid chromatography (HPLC) with ultraviolet light, diode-array detection (DAD), photodiode-array (PDA) detection (Bordagaray et al., 2013, 2014; Qi et al., 2014; Ma et al., 2016; Zhang Y. H. et al., 2016), gas chromatography (GC) with nitrogen-phosphorous detection (NPD) or electron capture detection (ECD) (Lozowicka et al., 2015; Im et al., 2016), and GC-mass spectrometry (GC-MS) (Tseng et al., 2014; Chu et al., 2015), and with tandem MS (GC-MS/MS) (Xu et al., 2013). Nevertheless, these chromatographic techniques necessitate experienced workers, costly devices, and lengthy specimen preparation. In comparison with the above-mentioned methods, spectrofluorimetry is the most favorable analytical strategy employed to analyze different biological specimens due to its innate simplicity, high sensitivity, and accessibility in the majority of quality-control and clinical laboratories (Yao et al., 2013). However, determination

of the existence of many common triazoles cannot be performed directly using typical fluorimetric techniques since the aqueous solutions with triazoles do not have native fluorescence.

It is noteworthy that the complexation of a fluorescent dye with a macrocycle host can induce significant change in its fluorescence (Zhou et al., 2008; Zhang et al., 2012; Kogawa et al., 2014). Such assays depend on an indicator-displacement technique in which the analyte competitively supplants a fluorescent guest that results in an alteration in its fluorescence intensity (You et al., 2015; Sayed and Pal, 2016). Various macrocyclic compounds, including cyclodextrins, calix[*n*]arenes, and pillar[*n*]arenes, have long been employed as the hosts in several macrocyclic-dye supramolecular systems (Choudhury et al., 2010; Lau and Heyne, 2010; Liu et al., 2015b; Sun et al., 2015). In particular, cucurbit[*n*]urils (Q[*n*]s) are made up of *n* glycoluril units connected via 2*n* methylene bridges (Day et al., 2000; Kim et al., 2000; Cong et al., 2016). These hosts have highly polar carbonyl-fringed portals with hydrophobic cavities that can create remarkably stable complexes with different guest molecules (Kim, 2002; Dsouza et al., 2011; Gao et al., 2017; Liu J. et al., 2017; Murray et al., 2017; Yang et al., 2018). The origination of inclusion complexes frequently improves or interrupts the photo-physical and photo-chemical characteristics of the guest molecules. For example, using different Q[*n*]s to encapsulate some dyes can change the fluorescent characteristics of the guest molecules (Praetorius et al., 2008; Baumes et al., 2009, 2011; Choudhury et al., 2009). The dye@Q[*n*] complexes can be composed of supramolecular fluorescent probes with high sensitivity and selectivity to recognize and detect analytes, such as metal ions, amines, pesticides, drugs, and DNA (Wheate, 2008; Mohanty et al., 2009; Nau et al., 2009; Zhou et al., 2009; Day and Collins, 2012; Xing et al., 2013; Elbashir and Aboul-Enein, 2015; Liu W. Q. et al., 2017; Xi et al., 2017; Tang et al., 2018; Wang et al., 2018).

Thioflavin T, 3,6-dimethyl-2-(4-dimethylaminophenyl) benzthiazolium cation (ThT) is a benzthiazolium dye (Figure 1). An aqueous solution of ThT reveals a weak native fluorescence. Nevertheless, as revealed by previous evaluations, the fluorescence of ThT in an aqueous solution can be vastly improved in the presence of Q[7], Q[8], and twisted cucurbit[14]uril (tQ[14]). It was found that ThT can form ThT@Q[*n*] inclusion complexes with different stoichiometric ratios, which can be applied to identify both alkali-metal and alkaline-earth-metal ions (Choudhury et al., 2009, 2010; Mohanty et al., 2009; Wang et al., 2018). In the present study, a procedure was proposed to determine the residues of triazole fungicides, such as azaconazole, triadimefon, tebuconazole, tricyclazole, flutriafol, penconazole, and triadimenol isomer A in aqueous solution (Figure 1).

RESULTS AND DISCUSSION

Fluorescence Quenching of ThT@tQ[14] With Flusilazole

Previous studies have proven that the fluorescence of ThT in an aqueous solution over a wide range of interaction ratios can be enhanced by its interaction with tQ[14] via different

interaction models due to the multiple cavity features of the tQ[14] molecule and two active moieties (the benzothiazole and dimethylaminobenzene moieties) in ThT (Wang et al., 2018). In the current work, we focused on the inclusion complexes of ThT@tQ[14] with 1:1 and 1:5 interaction ratios in the presence of the eight selected triazoles, the corresponding fluorescence spectra of which can be seen in Figure 2 and Figures S1–S3. A significant fluorescence quenching of the ThT@tQ[14] inclusion complex probe (1:1) was only observed upon increasing the amount of flusilazole; ~60% of the fluorescence intensity was lost when $C_{\text{flusilazole}}/C_{\text{ThT@tQ[14]}}$ was ~4 (Figure 2A). Figure 2B shows the plot of the fluorescence intensity at $\lambda_{\text{em}} = 488 \text{ nm}$ upon increasing the flusilazole concentration; K_{observed} was calculated by the nonlinear-least-squares method to be $(8.2 \pm 0.4) \times 10^5 \text{ L/mol}$ obtained (Figure S4), which is likely due to the influence of the interaction of tQ[14] with flusilazole on the interaction of tQ[14] with ThT. Moreover, the ThT@tQ[14] fluorescent probe presented high selectivity for flusilazole because the probe showed little or almost no response to the other seven triazole fungicides studied (Figure 3 and Figure S1). The ThT@tQ[14] inclusion complex probe at a molar ratio of 1:5 was also selected to investigate its response to triazole pesticides with the addition of flusilazole also leading to a fluorescence quenching of the ThT@tQ[14] inclusion complex probe; only ~22% of the fluorescence intensity was lost when $C_{\text{flusilazole}}/C_{\text{ThT@tQ[14]}}$ was ~4 (Figure S2). However, the ThT@tQ[14] fluorescent probe also showed little or almost no response to the other triazole fungicides studied (Figure S3).

Analytical Characteristics of ThT@tQ[14] Probe

The standard calibration curve (Figure S5) of the complexes of flusilazole with ThT@tQ[14] (1:1) was obtained using the plot of fluorescence intensity *F* compared to flusilazole concentration. The linear range was $(0.0\text{--}1.0) \times 10^{-6} \text{ mol/L}$ for flusilazole with a correlation coefficient of 0.9888. For flusilazole, the limit of detection (LOD) was $1.27 \times 10^{-8} \text{ mol/L}$ and the linear regression equation $F = -216.24C + 576.26$. Although the ThT@tQ[14] (1:5) inclusion complex was less sensitive to flusilazole, it still exhibited a very low LOD ($2.80 \times 10^{-8} \text{ mol/L}$) and the linear regression equation was $F = -98.25C + 863.26$ (Figure S6).

Effects of Interfering Substances

In the present work, the impacts of different common interfering substances on the determination of flusilazole using the ThT@tQ[14] probe were also investigated. The tolerance limit was established as the concentration of an added interfering substance that causes a relative error of $< \pm 5\%$ in the flusilazole determination. The samples consisted of a fixed amount of flusilazole ($1.0 \mu\text{M}$) and ThT@tQ[14] ($1.0 \mu\text{M}$) with an increasing amount of different interfering substances; the corresponding results are shown in Table 1 and Figure S7. It is clear that the determination was free from interference in the presence of the common metal ions and anions in aqueous solutions, except Ca^{2+} . Structural analysis revealed that tQ[14] had a similar portal size to those of Q[6] and

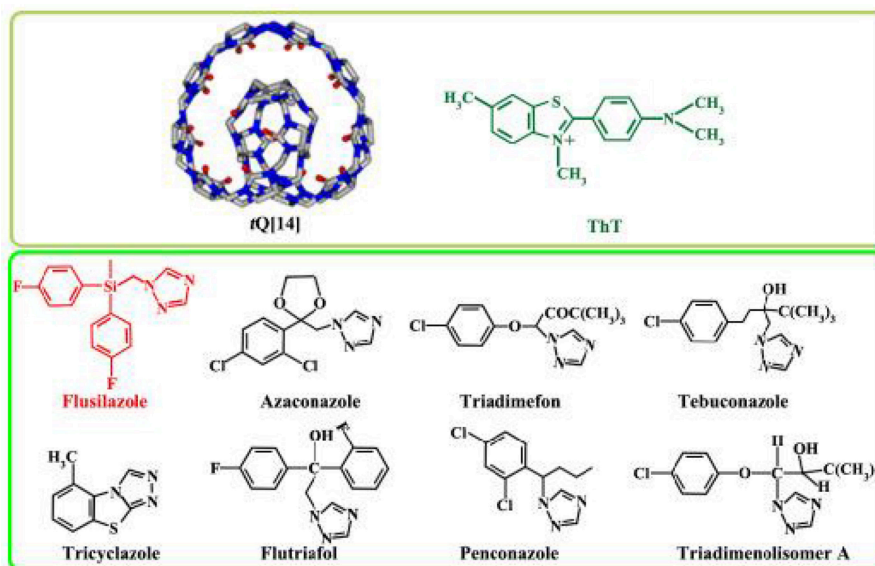


FIGURE 1 | Structures of tQ[14], ThT, and eight fungicide triazoles, namely flusilazole, azaconazole, triadimefon, tebuconazole, tricyclazole, flutriafol, penconazole, and triadimenol isomer A.

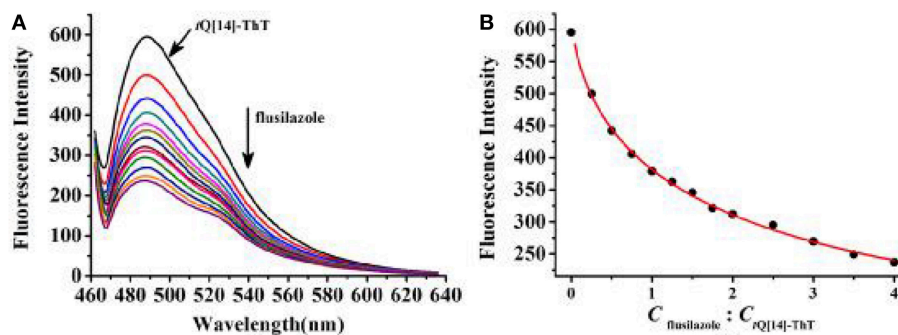


FIGURE 2 | (A) Fluorescence titration spectra ($\lambda_{ex} = 448$ nm) for ThT@tQ[14] (1:1, 1 μ M) in the presence of flusilazole of the following different stoichiometries in μ M: 0, 0.25, 0.5, 0.75, 1.0, 1.25, 1.5, 1.75, 2.0, 2.5, 3.0, 3.5, and 4.0; (B) Plot obtained for fluorescence intensity of ThT@tQ[14] vs. $C_{\text{flusilazole}}/C_{\text{ThT@tQ[14]}}$.

Q[7] (Cheng et al., 2013; Liu et al., 2015a; Li et al., 2016; Zhang J. et al., 2016; Zhang et al., 2017), and a higher portal carbonyl intensity (Cheng et al., 2013; Liu et al., 2015a; Zhang J. et al., 2016; Zhang et al., 2017), which could exhibit a higher affinity for metal cations, particularly the Ca^{2+} cation (Cheng et al., 2013; Qiu et al., 2017; Wang et al., 2018). The titration fluorescence spectra recorded for the tQ[14]-ThT-flusilazole (1:1:1) system upon increasing the amount of Ca^{2+} showed that the fluorescence of the ternary interaction system could be further decreased due to the influence of the Ca^{2+} cation (Figure S8). The titration ^1H nuclear magnetic resonance (NMR) spectra for the tQ[14]-ThT-flusilazole (1:1:1) system in the presence of Ca^{2+} also showed that the guest molecules, ThT and flusilazole, were gradually pushed out from the cavity area upon increasing the amount of Ca^{2+} (Figure S9).

Preliminary Exploration of the Response Mechanism of ThT@tQ[14] Fluorescent Probe Toward Flusilazole Titration ^1H NMR Spectra

We have found that the ThT@tQ[14] fluorescent probe was selectively sensitive toward flusilazole and could be used to detect flusilazole via a significant fluorescence quenching process. Why is the ThT@tQ[14] fluorescent probe selectively sensitive to flusilazole? How does the flusilazole molecule influence the interaction between the ThT molecule with the tQ[14] host molecule? What could the interaction mode be? To understand the selectivity and response mechanism of the ThT@tQ[14] fluorescent probe toward flusilazole, titration ^1H NMR spectra were recorded upon the gradual addition of one of the selected triazole fungicides into the solution of the ThT@tQ[14] (1:1) fluorescent probe. The detailed interaction of ThT and tQ[14]

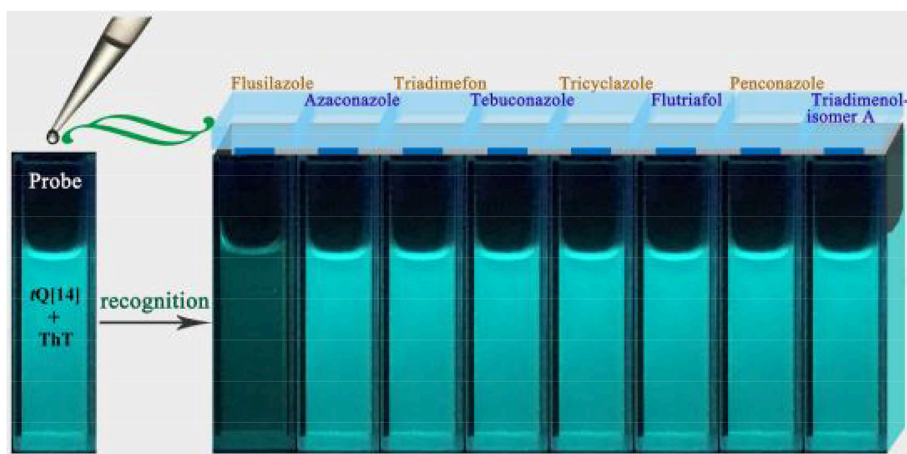


FIGURE 3 | Fluorescence images of ThT@tQ[14] (50 μ M) upon addition of eight triazole pesticides (50 μ M) under UV-lamp irradiation (365 nm).

TABLE 1 | Impact of interfering substances (tolerance error \pm 5%).

Interfering	Tolerance (mol/L)	Relative error (%)
Na ⁺	6.0×10^{-5}	-3.38
K ⁺	5.0×10^{-5}	-1.94
Zn ²⁺	1.0×10^{-3}	-2.65
Mg ²⁺	1.0×10^{-3}	-2.45
Cu ²⁺	5.0×10^{-5}	-4.67
Cl ⁻	4.0×10^{-5}	-3.97
Br ⁻	5.0×10^{-5}	-1.38
NO ₃ ⁻	6.0×10^{-5}	-4.63
HSO ₄ ⁻	5.0×10^{-5}	-1.38
H ₂ PO ₄ ⁻	4.0×10^{-5}	-2.77

has been discussed in a previous work (Figures 4A,B) (Wang et al., 2018). Figure 4F shows the ¹H NMR spectrum for the flusilazole in the presence of tQ[14]. When compared with the ¹H NMR spectrum for the unbound flusilazole molecule (Figure 4G), the proton resonances corresponding to H5 and H6 on the triazole moiety of the bound flusilazole molecule underwent slightly down-field shifts (0.01 and 0.01 ppm, respectively), whereas the other proton resonances experienced slightly up-field shifts, suggesting that a weak interaction existed between tQ[14] and the flusilazole guest molecule or $\pi \cdots \pi$ stacking of the aryl groups of the flusilazole guest molecules. Figures 4C–E show the titration ¹H NMR spectra for the tQ[14]-ThT complex upon increasing the amount of flusilazole. The addition of flusilazole appeared to pull the bound ThT out of the interaction area of the tQ[14] host because the proton resonances were closer to those of the unbound ThT molecule. However, the proton resonances of flusilazole, in particular, the H5 and H6 experienced down-field shift, suggesting that ThT was still interacting with the host and flusilazole was located in the de-shielding region of tQ[14] (probably at portal area). Similar phenomena could be observed for the other tQ[14]-ThT-triazole fungicide systems, in which the addition of the triazole fungicide

could lead to a change in the interaction between tQ[14] and ThT. Moreover, both ThT and the triazole fungicide exhibited an interaction with the tQ[14] host (Figures S10–S16). At first, it seemed that it was difficult to obtain the required information using the titration ¹H NMR method. A closer inspection revealed that the addition of different triazole fungicides could lead to different chemical shifts for the proton resonances corresponding to the ThT molecule, and the effects of the different triazole fungicides on the bound ThT were compared with the chemical shift corresponding to proton Hg. The data in Table 2 reveal that flusilazole resulted in the larger change in the chemical-shift values ($\Delta\delta = 0.05$) when the tQ[14]-ThT-triazole fungicide ratio was 1:1:2.

2D diffusion-ordered NMR spectroscopy (DOSY) experiments were performed to afford further evidence for the formation of the tQ[14]-ThT-flusilazole (1:1:1) ternary interaction species. Figure S17 depicts the DOSY spectra of tQ[14], ThT, flusilazole, and tQ[14]-ThT-flusilazole (1:1:1) ternary interaction species in D₂O at 298 K and the corresponding diffusion coefficients (D) are 3.49×10^{-10} , 5.46×10^{-10} , 3.88×10^{-10} , and 2.92×10^{-10} , respectively. According to the values of four species, the tQ[14]-ThT-flusilazole (1:1:1) ternary interaction species is the smallest, suggesting that the ternary species could be the largest species, moreover, all the proton signals of the host and the guest display the same diffusion coefficient ($D = 2.92 \times 10^{-10} \cdot \text{m}^2 \cdot \text{s}^{-1}$), indicating that they are part of the same species.

Isothermal Titration Calorimetry

Isothermal titration calorimetry (ITC) experiments were conducted to determine the association constants and thermodynamic parameters of the host-guest interaction between tQ[14] and ThT with the triazole fungicides in an aqueous solution to further explore the fluorescence-quenching mechanism of ThT@tQ[14] with flusilazole (Figures S18–S26). From the data acquired (Table 3), all the association constants obtained for the triazole fungicides@tQ[14] complexes

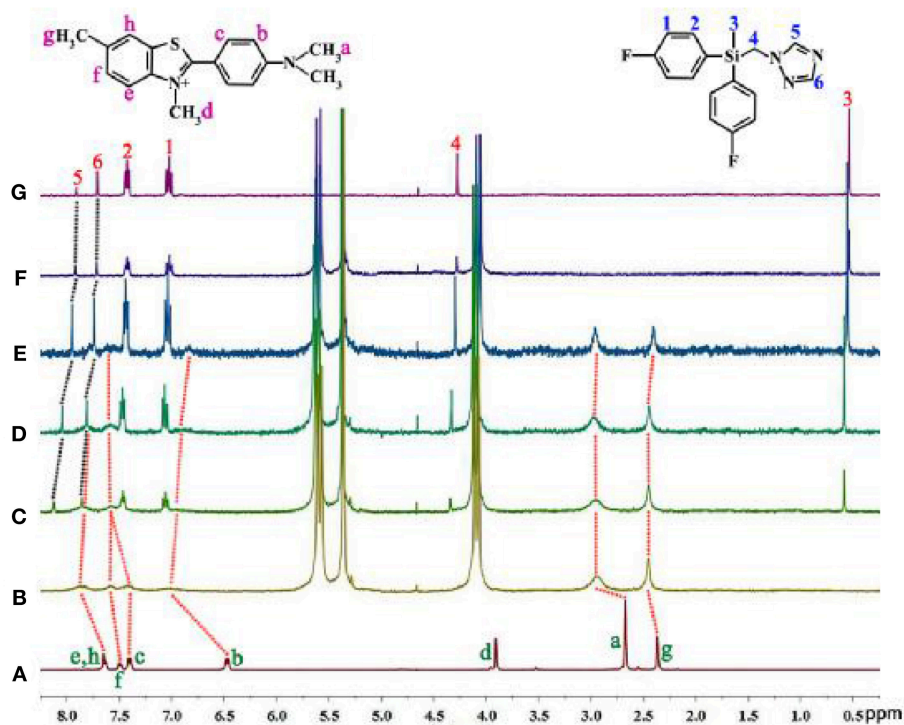


FIGURE 4 | ^1H NMR spectra (400 MHz, D_2O) for (A) ThT, (B) tQ[14]-ThT (1:1), (C) tQ[14]-ThT-flusilazole (1:1:0.5), (D) tQ[14]-ThT-flusilazole (1:1:1), (E) tQ[14]-ThT-flusilazole (1:1:2), (F) tQ[14]-flusilazole, and (G) flusilazole.

TABLE 2 | Chemical shifts corresponding to proton Hg of ThT.

Guest	δ [Q14-ThT (1:1)]	δ [Q14-ThT-G (1:1:2)]	$\Delta\delta$
Flusilazole	2.469	2.419	0.050
Azaconazole	2.453	2.439	0.014
Triadimefon	2.458	2.429	0.029
Tebuconazole	2.449	2.422	0.027
Tricyclazole	2.450	2.432	0.018
Flutriafol	2.453	2.429	0.024
Penconazole	2.451	2.430	0.021
Triadimenol isomer A	2.457	2.437	0.020

[[1.46–8.39) $\times 10^5$ L/mol] were slight larger than that of the ThT@tQ[14] complex (1.28×10^5 L/mol), but there are no significant differences. The titration ^1H NMR study has proved that these pesticides could not replace ThT to form pesticide@tQ[14] inclusion complexes.

The fluorescence enhancement mechanism of ThT could be due to the restriction of the freely rotating dimethylamine group on the benzene moiety, making the lone pair electrons on nitrogen atoms conjugate to the ThT aromatic system. The shell-like cavity structure of tQ[14] can provide such controlled environment, the inclusion of dimethylamino phenyl moiety of ThT inhibited dimethylamino free rotation, moreover, the shell-like cavity structure of tQ[14] could prevent ThT from threading through the side cavity of tQ[14] (Liu et al., 2015a;

TABLE 3 | Thermodynamic parameters of tQ[14] and ThT with eight triazole pesticides in aqueous solution at 298.15 K.

Complex	K_a (m^{-1})	ΔH (kJ/mol)	$T\Delta S$ (kJ/mol)
tQ[14]-ThT	$(1.28 \pm 0.03) \times 10^5$	-48.4	-19.2
tQ[14]-flusilazole	$(8.39 \pm 0.05) \times 10^5$	-38.4	-4.6
tQ[14]-azaconazole	$(5.45 \pm 0.08) \times 10^5$	-36.8	-4.0
tQ[14]-triadimefon	$(1.46 \pm 0.04) \times 10^5$	-64.3	-34.9
tQ[14]-tebuconazole	$(3.00 \pm 0.09) \times 10^5$	-42.7	-11.4
tQ[14]-tricyclazole	$(5.01 \pm 0.12) \times 10^5$	-36.8	-4.2
tQ[14]-flutriafol	$(1.97 \pm 0.05) \times 10^5$	-64.6	-34.3
tQ[14]-penconazole	$(5.23 \pm 0.08) \times 10^5$	-38.8	-6.2
tQ[14]-triadimenol isomer A	$(4.31 \pm 0.10) \times 10^5$	-39.0	-6.9

Li et al., 2016). Therefore, we can observe ThT fluorescence enhancement. Unlike HMeQ[6] and Q[7] which have similar portal sizes to that of the side portals of tQ[14], ThT could thread through their cavities, and show a weak fluorescence emission (referring the fluorescence spectra as shown in Figure S27). On the other hand, the fluorescence emission of ThT is also affected by its electron-pushing group (dimethylamine group) and electron-withdrawing group (quaternary ammonium moiety). The titration ^1H NMR spectra could provide the interaction images of this ternary system: the flusilazole was located in the deshielding region of tQ[14] (probably at portal area), which caused the chemical shift change of ThT proton resonance to move

toward the free ThT, in particular, the interaction of the azole moiety and quaternary ammonium moiety could weaken the electron-withdrawing capacity of quaternary ammonium moiety, resulting in partial quenching of the fluorescence of the *t*Q[14]-ThT-flusilazole interaction system (Figure 5). According to the suggested interaction mode, whether the fluorescence quenching of ThT@*t*Q[14] is caused mainly depends on the interaction of the azole moiety of pesticides and quaternary ammonium moiety of ThT and the ability of pesticides to pull ThT out of the side cavity of *t*Q[14]. While the NMR and ITC measurement results showed that the flusilazole has the biggest impact, although the differences from other triazole fungicides are subtle.

CONCLUSIONS

In order to further expand the application of Q[*n*]-based host-guest chemistry, especially the host-guest complexes with fluorescent properties, in detection and recognition, a known host-guest complex of ThT@*t*Q[14] (1:1) was used as a fluorescent probe to determine non-fluorescence triazole fungicides, including flusilazole, azaconazole, triadimefon, tebuconazole, tricyclazole, flutriafol, penconazole, and triadimenol isomer A. This new and simple fluorometry method proved to be highly selective and sensitive to one of triazole fungicides—flusilazole, and the determination was free from interference by the common metal ions and anions in aqueous solutions, except Ca²⁺. The investigation of the response mechanism revealed that a side-cavity of the *t*Q[14] host includes the dimethylamino phenyl moiety of ThT, resulting in the ThT fluorescence enhancement; the addition of flusilazole results in the interaction of the azole moiety of flusilazole and quaternary ammonium moiety of ThT, which could weaken

the electron-withdrawing capacity of quaternary ammonium moiety, resulting in partial quenching of the fluorescence of the *t*Q[14]-ThT-flusilazole interaction system. This unusual phenomenon results from the novel structural feature of *t*Q[14], namely that *t*Q[14] possesses a central-cavity and two of the same side-cavities.

EXPERIMENT

Materials

*t*Q[14] was set up and purified in our laboratory according to a procedure detailed in the literature (Cheng et al., 2013). Analytical grade flusilazole (99.5%), azaconazole (99.5%), triadimefon (99.0%), tebuconazole (99.0%), tricyclazole (99.0%), flutriafol (98.6%), penconazole (99.5%), and triadimenol isomer A (95.4%) were purchased from Dr. Ehrenstorfer GmbH (Augsburg, Germany) and used as-received without any further purification. Double-distilled water was used for each of the experiments.

¹H NMR

Each of the ¹H NMR spectra, including those for titration experiments, were documented at 25°C on a JEOL JNM-ECZ400s spectrometer using SiMe₄ as an internal reference. D₂O was utilized as a field-frequency lock and the chemical shifts documented in parts per million (ppm).

ITC

Microcalorimetric experiments were conducted with a Nano ITC (TA, USA) isothermal titration calorimeter. Then, 25 consecutive 10-μL aliquots of a 1 mM *t*Q[14] solution were introduced into the microcalorimetric reaction cell, which contained 1.3 mL of a 0.1-mM guest molecule solution at 25°C. The heat of reaction was

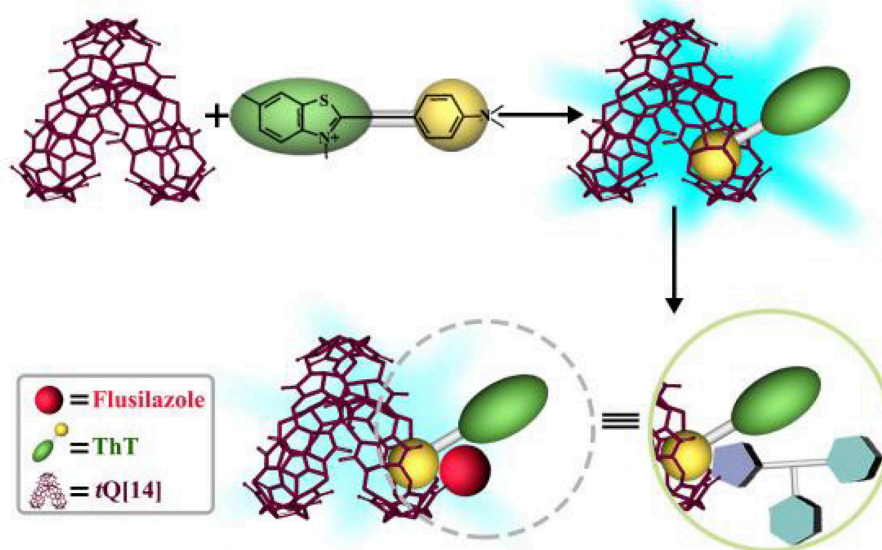


FIGURE 5 | Possible response mechanism for fluorescent probe ThT@*t*Q[14] with flusilazole.

corrected for the heat of dilution of the guest molecule solution, which was determined in a separate experiment. Each of the solutions were de-gassed before the titration via ultrasonication. Computer simulations (curve fitting) were conducted with Nano ITC analysis software.

Fluorescence Titration

The fluorescence spectra of the host-guest complexes were documented at 25°C using a Varian Cary Eclipse spectrofluorometer (Varian, Inc., Palo Alto, CA, USA). Stock solutions of tQ[14] (1×10^{-3} mol L⁻¹), ThT (1×10^{-3} mol L⁻¹), and flusilazole (1×10^{-4} mol L⁻¹) were set up in water. Working solutions were set up by diluting the stock solutions to the necessary concentrations.

A tQ[14]-ThT (1:1) complex solution was set up at a fixed concentration of 1×10^{-6} mol·L⁻¹ in H₂O, which was subsequently combined with flusilazole at guest/host ratios of 0, 0.25:1, 0.5:1, 0.75:1, 1:1, ..., and 4:1. Fluorescence spectrophotometric titrations were established as detailed prior ($\lambda_{\text{ex}} = 448$ nm and $\lambda_{\text{em}} = 488$ nm). For each experiment, three replicate measurements were recorded.

LOD Measurement

The calculation technique used for the LOD was based on the standard derivation of 10 measurements without the guest molecule (σ) and the slope of the linear calibration curve (K) based on the formula $LOD = 3\sigma/K$.

REFERENCES

- Baumes, L. A., Buaki, M., Jolly, J., Corma, A., and Garcia, H. (2011). Fluorimetric detection and discrimination of α -amino acids based on tricyclic basic dyes and cucurbiturils supramolecular assembly. *Tetrahedron Lett.* 52, 1418–1421. doi: 10.1016/j.tetlet.2011.01.071
- Baumes, L. A., Sogo, M. B., Montes-Navajas, P., Corma, A., and Garcia, H. (2009). First colorimetric sensor array for the identification of quaternary ammonium salts. *Tetrahedron Lett.* 50, 7001–7004. doi: 10.1016/j.tetlet.2009.09.165
- Bordagaray, A., García-Arrona, R., and Millán, E. (2013). Development and application of a screening method for triazole fungicide determination in liquid and fruit samples using solid-phase microextraction and HPLC-DAD. *Anal. Methods* 5, 2565–2571. doi: 10.1039/c3ay26433e
- Bordagaray, A., García-Arrona, R., and Millán, E. (2014). Determination of triazole fungicides in liquid samples using ultrasound-assisted emulsification microextraction with solidification of floating organic droplet followed by high-performance liquid chromatography. *Food Anal. Methods* 7, 1195–1203. doi: 10.1007/s12161-013-9733-2
- Cheng, X. J., Liang, L. L., Chen, K., Ji, N. N., Xiao, X., Zhang, J. X., et al. (2013). Twisted cucurbit[14]uril. *Angew. Chem. Int. Ed.* 52, 7252–7255. doi: 10.1002/anie.201210267
- Choudhury, S. D., Mohanty, J., Pal, H., and Bhasikuttan, A. C. (2010). Cooperative metal ion binding to a cucurbit[7]uril-thioflavin T complex: demonstration of a stimulus-responsive fluorescent supramolecular capsule. *J. Am. Chem. Soc.* 132, 1395–1401. doi: 10.1021/ja908795y
- Choudhury, S. D., Mohanty, J., Upadhyaya, H. P., Bhasikuttan, A. C., and Pal, H. (2009). Photophysical studies on the noncovalent interaction of thioflavin T with cucurbit[n]uril macrocycles. *J. Phys. Chem. B* 113, 1891–1898. doi: 10.1021/jp8103062
- Chu, S. P., Tseng, W. C., Kong, P. H., Huang, C. K., Chen, J. H., Chen, P. S., et al. (2015). Up-and-down-shaker-assisted dispersive liquid-liquid microextraction coupled with gas chromatography-mass spectrometry for the determination of fungicides in wine. *Food Chem.* 185, 377–382. doi: 10.1016/j.foodchem.2015.04.015
- Cong, H., Ni, X. L., Xiao, X., Huang, Y., Zhu, Q. J., Xue, S. F., et al. (2016). Synthesis and separation of cucurbit[n]urils and their derivatives[J]. *Org. Biomol. Chem.* 14, 4335–4364. doi: 10.1039/C6OB00268D
- Day, A. I., Arnold, A. P., and Blanch, R. J. (2000). Method for synthesis of cucurbiturils. *PCT Int. Appl.* 112.
- Day, A. I., and Collins, J. G. (2012). Cucurbituril receptors and drug delivery. *Supramol. Chem.* 3, 983–1000. doi.org/10.1002/9780470661345.smc056
- Dsouza, R. N., Pischel, U., and Nau, W. M. (2011). Fluorescent dyes and their supramolecular host-guest complexes with macrocycles in aqueous solution. *Chem. Rev.* 111, 7941–7980. doi: 10.1021/cr200213s
- Elbashir, A., and Aboul-Enein, H. Y. (2015). Supramolecular analytical application of cucurbit[n]urils using fluorescence spectroscopy. *Crit. Rev. Anal. Chem.* 45, 52–61. doi: 10.1080/10408347.2013.876354
- Fu, Y., Yang, T., Zhao, J., Zhang, L., Chen, R. X., and Wu, Y. L. (2017). Determination of eight pesticides in *Lycium barbarum* by LC-MS/MS and dietary risk assessment. *Food Chem.* 218, 192–198. doi: 10.1016/j.foodchem.2016.09.014
- Gao, R. H., Chen, L. X., Chen, K., Tao, Z., and Xiao, X. (2017). Development of hydroxylated cucurbit[n]urils, their derivatives and potential applications. *Coordinat. Chem. Rev.* 348, 1–24. doi: 10.1016/j.ccr.2017.07.017
- García-Valcárcel, A. I., and Tadeo, J. L. (2011). Determination of azoles in sewage sludge from Spanish wastewater treatment plants by liquid chromatography-tandem mass spectrometry. *J. Sep. Sci.* 34, 1228–1235. doi: 10.1002/jssc.201000814
- Im, S. J., Rahman, M. M., El-Aty, A. M. A., Kim, S. W., Kabir, H., Farha, W., et al. (2016). Simultaneous detection of fluquinconazole and flusilazole in lettuce using gas chromatography with a nitrogen phosphorus detector: decline patterns at two different locations. *Biomed. Chromatogr.* 30, 946–952. doi: 10.1002/bmc.3634
- Kim, J., Jung, I. S., Kim, S. Y., Lee, E., Kang, J. K., Sakamoto, S., et al. (2000). New cucurbituril homologues: syntheses, isolation, characterization, and X-ray

The standard deviation of 10 measurements without the guest molecule could be determined based on the following relationship: $\sigma = \sqrt{\frac{1}{n-1} \sum_{i=1}^n (x_i - \bar{x})^2}$, where n is the number of measurements ($n = 11$).

AUTHOR CONTRIBUTIONS

YF, R-HG, YH, and BB undertook the acquisition and analysis of data for the work. ZT and XX drafted the work and revised it critically for important intellectual content.

ACKNOWLEDGMENTS

We acknowledge the support of the National Natural Science Foundation of China (Grant No. 21562015), the Creative Research Groups of Guizhou Provincial Education Department (2017-028), and the Innovation Program for High-level Talents of Guizhou Province (No. 2016-5657).

SUPPLEMENTARY MATERIAL

The Supplementary Material for this article can be found online at: <https://www.frontiersin.org/articles/10.3389/fchem.2019.00154/full#supplementary-material>

- crystal structures of cucurbit[n]uril ($n = 5, 7, \text{ and } 8$). *J. Am. Chem. Soc.* 122, 540–541. doi: 10.1021/ja993376p
- Kim, K. (2002). Mechanically interlocked molecules incorporating cucurbituril and their supramolecular assemblies. *Chem. Soc. Rev.* 31, 96–107. doi: 10.1039/a900939f
- Kogawa, C., Zoppi, A., Quevedo, M. A., Salgado, H. R. N., and Longhi, M. R. (2014). Increasing doxycycline hyclate photostability by complexation with beta-cyclodextrin. *AAPS PharmSciTech.* 15, 1209–1217. doi: 10.1208/s12249-014-0150-7
- Lau, V., and Heyne, B. (2010). Calix[4]arene sulfonate as a template for forming fluorescent thiazole orange H-aggregates. *Chem. Commun.* 46, 3595–3597. doi: 10.1039/c002128h
- Li, Q., Qiu, S. C., Chen, K., Zhang, Y., Wang, R. B., Huang, Y., et al. (2016). Encapsulation of alkyldiammonium ions within two different cavities of twisted cucurbit[14]uril. *Chem. Commun.* 52, 2589–2592. doi: 10.1039/C5CC08642F
- Liu, J., Lan, Y., Yu, Z. Y., Tan, C. S. Y., Parker, R. M., Abell, C., et al. (2017). Cucurbit[n]uril-based microcapsules self-assembled within microfluidic droplets: a versatile approach for supramolecular architectures and materials. *Acc. Chem. Res.* 50, 208–217. doi: 10.1021/acs.accounts.6b00429
- Liu, Q., Li, Q., Cheng, X. J., Xi, Y. Y., Xiao, B., Xiao, X., et al. (2015a). A novel shell-like supramolecular assembly of 4,4-bipyridyl derivatives and a twisted cucurbit[14]uril molecule. *Chem. Commun.* 51, 9999–10001. doi: 10.1039/C5CC02653A
- Liu, Q., Yang, Y., Li, H., Zhu, R., Shao, Q., Yang, S., et al. (2015b). NiO nanoparticles modified with 5,10,15,20-tetrakis(4-carboxyl phenyl)-porphyrin: promising peroxidase mimetics for H_2O_2 and glucose detection. *Biosens. Bioelectron.* 64, 147–153. doi: 10.1016/j.bios.2014.08.062
- Liu, W. Q., Samanta, S. K., Smith, B. D., and Isaacs, L. (2017). Synthetic mimics of biotin/(strept)avidin. *Chem. Soc. Rev.* 46, 2391–2403. doi: 10.1039/C7CS00011A
- Lozowicka, B., Abzeitova, E., Sagitov, A., Kaczynski, P., Toleubayev, K., and Li, A. (2015). Studies of pesticide residues in tomatoes and cucumbers from Kazakhstan and the associated health risks. *Environ. Monit. Assess.* 187:609. doi: 10.1007/s10661-015-4818-6
- Ma, J. P., Yao, Z. D., Hou, L. W., Lu, W. H., Yang, Q. P., Li, J. H., et al. (2016). Metal-organic frameworks (MOFs) for magnetic solid-phase extraction of pyrazole/pyrrole pesticides in environmental water samples followed by HPLC-DAD determination. *Talanta* 161, 686–692. doi: 10.1016/j.talanta.2016.09.035
- Mohanty, J., Choudhury, S. D., Upadhyaya, H. P., Bhasikuttan, A. C., and Pal, H. (2009). Control of the supramolecular excimer formation of thioflavin T within acurbit[8]uril host: a fluorescence on/off mechanism. *Chem. Eur. J.* 15, 5215–5219. doi: 10.1002/chem.200802686
- Murray, J., Kim, K., Ogoishi, T., Yao, W., and Gibb, B. C. (2017). The aqueous supramolecular chemistry of cucurbit[n]urils, pillar[n]arenes and deep-cavity cavitands. *Chem. Soc. Rev.* 46, 2479–2496. doi: 10.1039/C7CS00095B
- Nau, W. M., Ghale, G., Hennig, A., Bakirci, H., and Bailey, D. M. (2009). Substrate-selective supramolecular tandem assays: monitoring enzyme inhibition of arginase and diamine oxidase by fluorescent dye displacement from calixarene and cucurbituril macrocycles. *J. Am. Chem. Soc.* 131, 11558–11570. doi: 10.1021/ja904165c
- Praetorius, A., Bailey, D. M., Schwarzlose, T., and Nau, W. M. (2008). Design of a fluorescent dye for indicator displacement from cucurbiturils: a macrocycle-responsive fluorescent switch operating through a pK_a shift. *Org. Lett.* 10, 4089–4092. doi: 10.1021/ol8016275
- Qi, R. F., Jiang, H. C., Liu, S. X., and Jia, Q. (2014). Preconcentration and determination of pesticides with graphene-modified polymer monolith combined with high performance liquid chromatography. *Anal. Methods* 6, 1427–1434. doi: 10.1039/c3ay41688g
- Qiu, S. C., Chen, K., Wang, Y., Hua, Z. Y., Li, F., Huang, Y., et al. (2017). Crystal structure analysis of twisted cucurbit[14]uril conformations. *Inorg. Chem. Commun.* 86, 49–53. doi: 10.1016/j.inoche.2017.09.024
- Sayed, M., and Pal, H. (2016). Supramolecularly assisted modulations in chromophoric properties and their possible applications: an overview. *J. Mater. Chem. C* 4, 2685–2706. doi: 10.1039/C5TC03321G
- Sun, N. N., Xiao, X., Li, W., and Jiang, J. Z. (2015). Multi-stimuli sensitive behavior of novel bipyridyl-involved pillar[5]arene-based fluorescent [2]rotaxane and its supramolecular gel. *Adv. Sci.* 2, 1500082–1500090. doi: 10.1002/advs.201500082
- Tang, Q., Zhang, J., Sun, T., Wang, C. H., Huang, Y., Zhou, Q. D., et al. (2018). A turn-on supramolecular fluorescent probe for sensing benzimidazole fungicides and its application in living cell imaging. *Spectrochim. Acta Part A Mol. Biomol. Spectrosc.* 191, 372–376. doi: 10.1016/j.saa.2017.10.042
- Tseng, W. C., Chu, S. P., Kong, P. H., Huang, C. K., Chen, J. H., Chen, P. S., et al. (2014). Water with low concentration of surfactant in dispersed solvent-assisted emulsion dispersive liquid-liquid microextraction for the determination of fungicides in wine. *J. Agric. Food Chem.* 62, 9059–9065. doi: 10.1021/jf5036096
- Wang, H., Tang, Q., Zhang, J., Yao, Y. Q., Xiao, X., Huang, Y., et al. (2018). Alkaline earth cation-mediated photoluminescent complexes of thioflavin T with twisted cucurbit[14]uril. *N. J. Chem.* 42, 9244–9251. doi: 10.1039/C7NJ04115B
- Wheate, N. J. (2008). Improving platinum(II)-based anticancer drug delivery using cucurbit[n]urils. *J. Inorgan. Biochem.* 102, 2060–2066. doi: 10.1016/j.jinorgbio.2008.06.005
- Xi, Y. Y., Tang, Q., Huang, Y., Tao, Z., Xue, S. F., Zhou, Q. D., et al. (2017). A novel fluorescence indicator displacement assay for sensing the anticancer drug gefitinib. *Supramol. Chem.* 29, 229–235. doi: 10.1080/10610278.2016.1202413
- Xing, X. Q., Zhou, Y. Y., Sun, J. Y., Tang, D. B., Li, T., and Wu, K. (2013). Determination of paraquat by cucurbit[7]uril sensitized fluorescence quenching method. *Anal. Lett.* 46, 694–705. doi: 10.1080/00032719.2012.729240
- Xu, M., Lu, S. Y., Chen, D. J., Lan, J. C., G., Zhang, Z., et al. (2013). Determination of ten pesticides of pyrazoles and pyrroles in tea by accelerated solvent extraction coupled with gas chromatography-tandem mass spectrometry. *Chinese J. Chromatogr.* 31, 218–222. doi: 10.3724/SP.J.1123.2012.10003
- Yang, L. G., Kan, J. L., Wang, X., Zhang, Y. H., Tao, Z., Liu, Q. Y., et al. (2018). Study on the binding interaction of the $\alpha, \alpha', \delta, \delta'$ -tetramethylcucurbit[6]uril with biogenic amines in solution and the solid state. *Front. Chem.* 6:289. doi: 10.3389/fchem.2018.00289
- Yao, F. H., Liu, H. L., Wang, G. Q., Du, L. M., Yin, X. F., and Fu, Y. L. (2013). Determination of paraquat in water samples using a sensitive fluorescent probe titration method. *J. Environ. Sci.* 25, 1245–1251. doi: 10.1016/S1001-0742(12)60124-7
- You, L., Zha, D. J., and Anslin, E. V. (2015). Recent advances in supramolecular analytical chemistry using optical sensing. *Chem. Rev.* 115, 7840–7892. doi: 10.1021/cr5005524
- Zhang, H. Y., Liu, L. L., Gao, C., Sun, R. Y., and Wang, Q. C. (2012). Enhancing photostability of cyanine dye by cucurbituril encapsulation. *Dyes Pigm.* 94, 266–270. doi: 10.1016/j.dyepig.2012.01.022
- Zhang, J., Tang, Q., Gao, Z. Z., Huang, Y., Xiao, X., and Tao, Z. (2017). Stimuli-responsive supramolecular assemblies between twisted cucurbit[14]uril and hemicyanine dyes and their analysis application. *J. Phys. Chem. B* 121, 11119–11123. doi: 10.1021/acs.jpcc.7b10285
- Zhang, J., Xi, Y. Y., Li, Q., Tang, Q., Wang, R. B., Huang, Y., et al. (2016). Supramolecular recognition of amino acids by twisted cucurbit[14]uril. *Chem. Asian J.* 11, 2250–2254. doi: 10.1002/asia.201600803
- Zhang, Y. H., Zhang, Y., Zhao, Q. Y., Chen, W. J., and Jiao, B. N. (2016). Vortex-assisted ionic liquid dispersive liquid-liquid microextraction coupled with high-performance liquid chromatography for the determination of triazole fungicides in fruit juices. *Food Anal. Methods* 9, 596–604. doi: 10.1007/s12161-015-0223-6
- Zhou, Y. Y., Yu, H., Zhang, L., Xu, H. W., Wu, L., et al. (2009). A new spectrofluorometric method for the determination of nicotine base on the inclusion interaction of methylene blue and cucurbit[7]uril. *Microchim. Acta* 64, 63–68. doi: 10.1007/s00604-008-0032-3
- Zhou, Y. Y., Yu, H. P., Zhang, L., Sun, J. Y., Wu, L., Lu, Q., et al. (2008). Host properties of cucurbit[7]uril: fluorescence enhancement of acridine orange. *J. Inclusion Phenom. Macrocyc. Chem.* 61, 259–264. doi: 10.1007/s10847-008-9414-8

Conflict of Interest Statement: The authors declare that the research was conducted in the absence of any commercial or financial relationships that could be construed as a potential conflict of interest.

Copyright © 2019 Fan, Gao, Huang, Bian, Tao and Xiao. This is an open-access article distributed under the terms of the Creative Commons Attribution License (CC BY). The use, distribution or reproduction in other forums is permitted, provided the original author(s) and the copyright owner(s) are credited and that the original publication in this journal is cited, in accordance with accepted academic practice. No use, distribution or reproduction is permitted which does not comply with these terms.